

# INTERNATIONAL SOCIETY FOR SOIL MECHANICS AND GEOTECHNICAL ENGINEERING



*This paper was downloaded from the Online Library of the International Society for Soil Mechanics and Geotechnical Engineering (ISSMGE). The library is available here:*

<https://www.issmge.org/publications/online-library>

*This is an open-access database that archives thousands of papers published under the Auspices of the ISSMGE and maintained by the Innovation and Development Committee of ISSMGE.*

# Ground movements associated with deep excavation - characterization

C. S. Yoo & J. H. Kim

*Sungkyunkwan University, Suwon, Kyong-Gi Do, Korea*

**ABSTRACT:** This paper presents the results of numerical investigation on deep excavation-induced ground movements, which are of prime importance in the perspective of damage assessment of adjacent buildings. A finite element model, which can realistically replicate deep-excavation-induced ground movements was employed and validated against available large-scale model test results. The validated model was then used to perform a parametric study on deep excavations with emphasis on ground movements. Based on the results, important factors influencing ground movements and fundamental characteristics of wall and ground movements are identified. Normalized profiles, which can be readily used as a means for estimating ground surface displacements for cases with similar excavation geometry and ground condition, are presented.

## 1 INTRODUCTION

Due to rapid growth in urban development deep excavations for high-rise buildings and subway construction are in great demand. During deep excavation, changes in the state of stress in the ground mass around the excavation and subsequent ground losses inevitably occur. These changes in the stress and ground losses are reflected to surrounding ground in the form of ground surface movements, which eventually impose direct strains onto nearby structures through translation, rotation, and distortion. The magnitude and distribution of ground movements for a given excavation depend largely on soil properties, excavation geometry including depth, width, and length, and types of wall and support system, and more importantly construction procedures. Due to an increased public concern on the effects of construction related ground movements on their properties, prediction of ground movements and assessment of the risk of damage has become an essential part of the planning, design, and construction of a deep excavation project in the urban environments.

Ground surface movements associated with a deep excavation, which are of prime importance in the perspective of building damage assessment, have not been fully explored due in large part to difficulties in obtaining complete sets of data from either field instrumentation or numerical analysis. Due to limited accessibility of surrounding area during deep excavations in urban environments, well-documented ground movement data from which ground displacement profiles can be constructed are

scarce. In addition, numerical approaches, such as finite-difference or finite-element method, also have not been able to provide realistic ground surface movements, due primarily to problems associated with modeling of the components comprising the soil-wall-support system. Available information on the magnitude and distribution of ground surface movements for deep excavations, therefore, is somewhat out-dated and only provides part of information required for building damage assessment.

This study is directed toward development of a prediction method for deep excavation-induced ground movements that can be used when making first order estimate of building damage associated with deep-excavation using the available methods (Boscardin & Cording, 1987, Burland, 1995). A series of finite-element analyses were performed to identify sources of wall movements during deep excavations and the results were carefully analyzed in such a manner that the ground movement characteristics can be related to the sources of wall movements. Normalized ground surface displacement profiles, from which a first order prediction of deep excavation-induced ground surface displacements can be made, are presented.

## 2 SOURCES OF WALL MOVEMENTS DURING EXCAVATION

Ground movements associated with a deep excavation are closely related to movements of the excava-

tion wall in a characteristic manner. Primary sources of wall movements are identified and related to ground surface movement patterns.

### 2.1 Components of wall movements

During excavation, the soil removal causes lateral ground loss at the wall through wall deformation. The lateral wall movements are then distributed to the adjacent ground and realized on the ground surface, imposing strains to adjacent buildings. Therefore, the excavation-induced ground movements are directly related to the lateral wall movements.

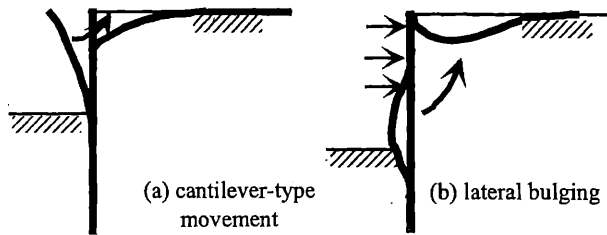


Figure 1. Components of wall movement.

Due to staged construction procedures adopted in deep excavations, each construction stage contributes to final patterns of wall and ground movements in a characteristic manner. For example, as illustrated in Figure 1a, the cantilever type wall movement occurs during early stages of excavation before supports are installed. Once upper levels of support are installed, the supports and the bottom of excavation provide resistance to wall deformation, and therefore, lateral bulging between the unsupported span becomes a primary source of wall movement (Figure 1b). The unsupported span length during excavation is, therefore, significantly related to the magnitude and the distribution of wall movements for a given excavation. The respective ground surface settlement profile for each component of wall movements exhibits a distinctive pattern, i.e., a parabolic shape for the cantilever-type movement and a concave downward shape for the lateral bulging. Final ground surface settlement profile for any deep excavation can thus be described once the contribution from each source of wall movements is identified. This is discussed further later in this paper. Although not discussed here, for walls supported by tiebacks, overall translation or outward rotation of the walls about the toe can occur with this component being more pronounced for walls with comparative stiffness. Such a pattern of wall deformation is more or less unique to tieback walls and is not discussed further.

A strategy for minimizing wall movement thus should be directed toward reducing the two sources of wall movements; the cantilever-type movement and the lateral bulging. The cantilever wall movement can be eliminated or reduced by either using stiffer walls or installing upper levels of support as early as possible. Obviously, a more economical

way would be the latter approach, which can be controlled during construction. In addition, the lateral bulging-induced wall movement can be reduced by enforcing a strict standard on the excavation depth below a lower-most support.

### 2.2 Flexibility ratio

It has been emphasized by Cording & O'Rourke (1977) and later by Cording (1985) that the lateral wall movement during excavation is significantly related to construction procedures. Cording & O'Rourke (1977) developed a scaling relation as Eq. (1) in evaluating the behavior of braced walls in dense soils based on elastic assumptions (Fig. 2). They employed the beam on elastic foundation theory to show that the lateral wall movement is greatly related to the maximum excavation depth,  $L$ , below a lower-most strut level. As seen in Figure 2, the lateral wall displacement due to the soil removal at an  $i^{\text{th}}$  excavation step can be viewed as the displacement  $y_c$  of a fixed-end beam subjected to uniform pressure  $q$ . Replacing the soil as a series of springs and employing the beam on elastic foundation concept, the displacement  $y_c$  can be expressed as Eq. (1)

$$y_c = \frac{qL}{E_s} \left[ 1 - 2 \left( \frac{\sinh \frac{\sqrt[4]{2F}}{2} \cos \frac{\sqrt[4]{2F}}{2} + \cosh \frac{\sqrt[4]{2F}}{2} \sin \frac{\sqrt[4]{2F}}{2}}{\sin \sqrt[4]{2F} + \sinh \sqrt[4]{2F}} \right) \right] \quad (1)$$

$$\text{where: } F = \frac{1}{8} \frac{E_s L^3}{EI}$$

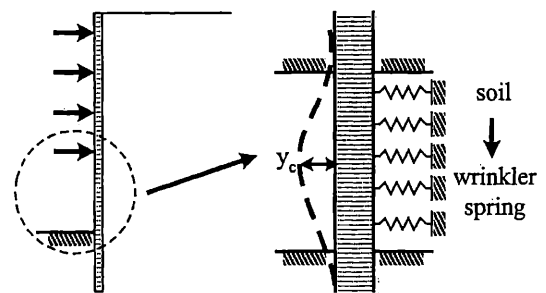


Figure 2. Modeling of lateral bulging

The parameter  $F$  is known as flexibility ratio indicating the relative stiffness of excavation wall with respect to soil stiffness. As one can expect, the maximum excavation depth  $L$  below a lower-most support has the greatest influence on the flexibility ratio and consequently on the wall movement since it is raised to the third power.

## 3 PARAMETRIC STUDY

A parametric study was performed using a finite-element model to identify sources of wall movements and to relate them to the patterns of ground

surface movement profiles. Subsequent sections discuss the details of the parametric study.

### 3.1 Problems investigated

Refer to Figure 3, for simplicity, an idealized (symmetric) plane strain braced excavation geometry with an excavation depth  $H$  and a width  $B$  of 20 and 30 m, respectively, was considered. The excavation site was assumed to be composed of layers of soil deposits overlying a rock stratum located at the final excavation platform.

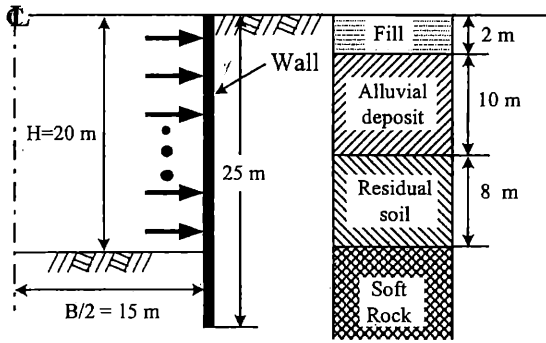


Figure 3. Excavation geometry

Primary variables considered include the wall bending stiffness  $(EI)_w$ , the cantilever excavation depth  $H_{un}$ , and the excavation depth  $L$  below a lower-most support. Relatively poor geotechnical characteristics were assumed for the soil deposits to represent rather potentially problematic situations in terms of wall and ground movements. A wide range of conditions was analyzed varying the primary variables mentioned above. Table 1 summarizes the conditions analyzed.

Table 1. Conditions analyzed

$(EI)_w$ (kN-m <sup>2</sup> /m)	$L$ (m)	$H_{un}$ (m)
17,50,150,430	4,5,6,7	1,2,3,4

### 3.2 Finite element modeling

A series of two-dimensional finite element analyses were performed using the commercial finite-element code ABAQUS (ABAQUS, 1999). ABAQUS was selected in this study due to its effectiveness in interface modeling as well as robustness in numerical solution strategy for soil plasticity.

In the finite element modeling, the ground and the wall were modeled using eight-noded plane strain elements (CPE8R) with  $8 \times 8$  integration, while the struts were modeled using one-node spring elements (SPRING1). A refined mesh, which consists of more than approximately 5800 nodes and 1870 elements, was adopted to minimize the effect of mesh dependency on the finite element modeling as shown in Fig. 4. Due to the symmetry about the excavation centerline, only one half of the excavation was considered in the finite element model. The finite element mesh extends to a depth of  $1.0H$  below the final excavation platform and laterally to a

distance of  $3.8H$  from the excavation centerline. Locations of these boundaries were selected in accordance with the results of preliminary analyses so that the presence of the artificial boundaries does not significantly alter the stress-strain field around the excavation.

The preliminary analysis indicated that the interface modeling of the excavation side is critical for realistic modeling of the ground movements associated with excavation, and therefore interfaces for both the retained and the excavation sides were modeled. Interface elements (INTER3) were used to model the interface between the wall and the ground. The inset in Figure 4 illustrates the modeling detail adopted in this study.

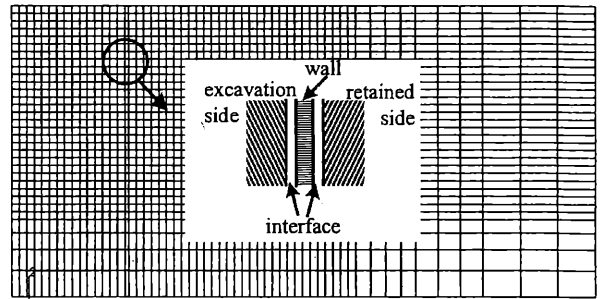


Figure 4. Finite element mesh

In the analysis, the soils were assumed to be elasto-plastic materials obeying the Extended Drucker-Prager failure criterion together with the non-associated flow rule proposed by Davis (1968), while the wall and the struts being a linear elastic material. The dilatancy angle  $\psi$  for a given soil was related to the friction angle  $\phi$  and the constant critical state friction angle  $\phi_{cv}$  using the assumption of Rowe's stress-dilatancy theory (Rowe, 1962) given by Eq. (2). The interface was modeled using an extended version of the classical isotropic Coulomb friction model, in which the friction coefficient is defined in terms of slip rate, contact pressure, average surface temperature at the contact point, and field variables. In this study, the interface was assumed to be dependent of contact pressure with a friction angle of 20 degrees. Table 2 shows the material properties adopted in this study

$$\sin \psi = \frac{\sin \phi - \sin \phi_{cv}}{1 - \sin \phi \sin \phi_{cv}} \quad (2)$$

Table 2. Material properties used

	$c$ (kPa)	$\phi$ (deg)	$\phi_{cv}$ (deg)	$\psi$ (deg)	$E_s$ (kPa)
fill	3	28	20	10	15,000
alluvial t	15	35	28	6	35,000
residual	50	38	32	6	50,000
soft rock	100	45	40	6	500,000

### 3.3 Model validation

Before proceeding the parametric study, the proposed finite-element model was validated against the

results of large-scale model test conducted at the University of Illinois. The model wall of 2.2 m in height with a 0.3 m of toe penetration consisted of soldier piles and lagging and was supported by two levels of tiebacks. Excavation and wall dimensions were generally selected to provide 1/4-scale models of typical tie-back walls. Excavation was carried out to a design grade of 1.9 m. Model soldier piles consisted of structural steel tubing with a rectangular cross-section and were placed on 0.6 m centers. A 0.3-cm-thick steel plate was used to simulate hardwood lagging. Tiebacks were modeled using small diameter (0.63 cm) steel bars, which were placed inside a flexible and extensible hose to isolate them from the surrounding soil mass. Figure 5 illustrates a schematic cross sectional view of the model test set-up.

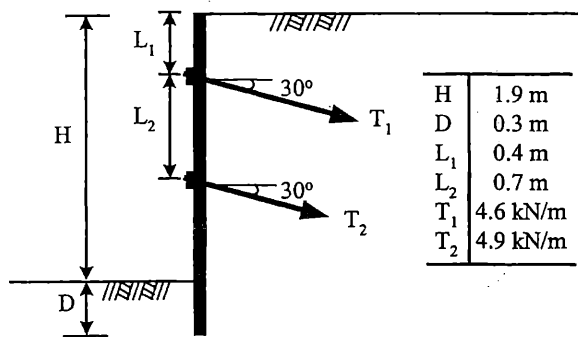


Figure 5. Model test configuration

Model soil used in the tests was a medium-grained, uniform sand classified SP according to the Unified Soil Classification System. Sand was placed inside the test pit by pluviation through air with a height of fall of approximately 1.2 m. Mechanical properties of the model soil and the wall components are summarized in Table 3. Details of the test instruments are available elsewhere (Mueller 2000). The finite element modeling approach was the same as the one described in the previous section, except that the wall and the tiebacks are modeled using beam (B22) and two-node spring (SPRING2) elements, respectively. In addition, the confining pressure-dependent soil modulus was taken into consideration by assigning different moduli at varying depths.

Figure 6 compares the results of the finite element analysis with those of the model test. Note that the results shown represent two stages; one for excavation to a depth of 0.5 m and the other for excavation to the design grade of 1.9 m. Note that the ground surface settlements from the model test appear to be slightly greater than those from the finite element analysis especially at the final stage. The variability of the ground surface settlements may have been caused by closure of small voids between the lagging and the ground. Nevertheless, the results of the finite-element analysis for the two stages of excavation compare fairly well with those from the model

test. It is also noted that the ground surface settlement profiles are characterized by a parabolic shape due to relatively flexible nature of the model wall. The result of the finite element analysis is consistent with this trend.

Table 3. Material properties used for model test simulation

	$\phi$ (deg)	$\phi_v$ (deg)	$\psi$ (deg)	$E_s$ (kPa)	$\gamma_s$ (kN/m <sup>3</sup> )
sand	40	35	6	$1234 \times (\sigma_1)^{0.5}$	18
wall bending stiffness	$(EI)_w = 14 \text{ kN-m}^2/\text{m}$				
tieback axial stiffness	$K = 28 \text{ kN/m}$				

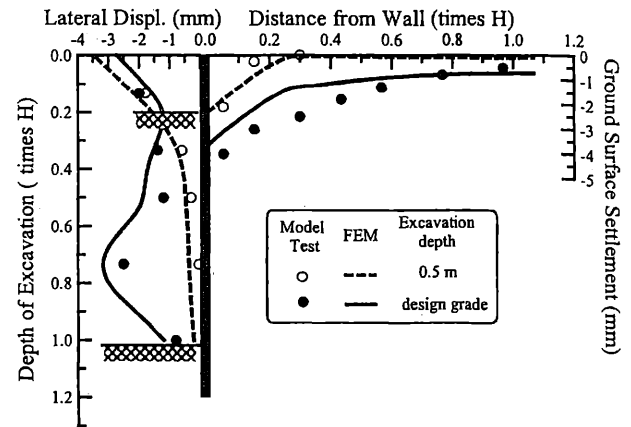


Figure 6. Comparison of finite element analysis and model test

## 4 GROUND MOVEMENT CHARACTERISTICS

The results of finite-element analyses were analyzed in a way that patterns of wall and ground movements can be related to the factors affecting the flexibility ratio. Important findings are discussed under the subsequent subheadings.

### 4.1 Effect of wall stiffness

Figure 7 demonstrates the effect of wall bending stiffness on the wall and ground surface movement patterns. FR is the flexibility ratio defined as  $FR = E_s L^3 / (EI)_w$ . Note that the excavation depth below a lower-most support was kept constant at  $L = 5$  m. As one might expect, an increase in the wall stiffness results in a decrease both in the lateral wall and ground surface movements. It is, however, of worth noting that the wall and ground surface movements profiles vary with  $(EI)_w$  in a characteristic manner. For example, the wall movement profiles for less stiff walls tend to show relatively large movement at the top due to the cantilever-type movement, and the resulting ground settlement profiles follow more or less a parabolic shape with a maximum value near the edge of excavation. As the wall stiffness increases, however, the lateral wall movements at the cantilever stages decrease significantly with which the lateral bulging becomes a dominant source of wall movements. The resulting ground settlement profiles take more or less a con-

cave downward shape with much reduced volume loss at the ground surface. The results shown in these figures suggest that the shapes of ground surface displacement profiles are significantly influenced by the wall stiffness, and that the cantilever-type wall movement at the top would considerably increase the volume of ground loss at the surface. Provisions must therefore be implemented to avoid potentially damaging ground movements by adopting stiffer walls and/or placing upper levels of support in early stages of excavation.

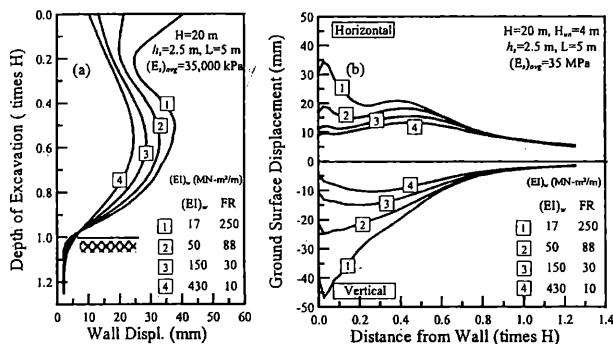


Figure 7. Variation of wall and ground movements with  $(EI)_w$ .

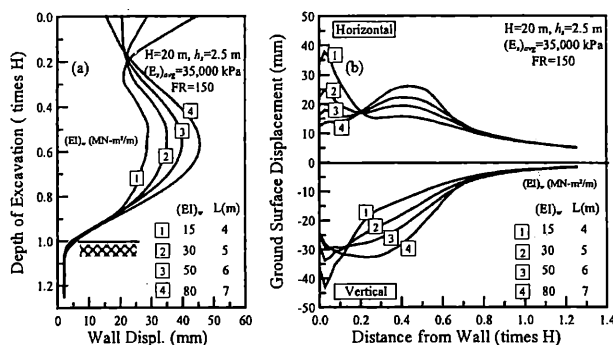


Figure 8. Variation of wall and ground movements with combined effect of  $(EI)_w$  and  $L$ .

Presented in Figure 8 are the results of four cases having the same flexibility ratio of  $FR=150$  but with different combinations of  $(EI)_w$  and  $L$ . The differences in the wall and ground movements between the cases represent the combined effect of the wall stiffness and the excavation depth  $L$ . As illustrated, the wall and ground movements for stiff walls with a large  $L$  are comparable to those for less stiff walls but with a small  $L$ . Moreover, it is evident that the extent to which significant ground surface loss occurs is greater for the cases with larger  $L$ , suggesting that the risk of damage associated with deep excavation is greater when allowing a large excavation depth  $L$  even for stiff walls. In view of minimizing the risk of damage, the excavation depth  $L$  appears to be far more important factor than the wall stiffness.

#### 4.2 Effect of construction procedure

The flexibility ratio, which is a measure of relative stiffness of a wall system, is greatly influenced by

the excavation depth  $L$ , since it is raised to the third power. The excavation depth  $L$  is somewhat related to construction procedures adopted for a given excavation, and can therefore be controlled to a large extent during construction. Both the cantilever-type movement and the lateral bulging are related to this issue and subsequent paragraphs discuss how these affect the patterns of surface ground movements.

As mentioned earlier, significant portion of wall movements develops during the cantilever stages of excavation, especially for flexible walls, such as sheet pile or soldier pile walls. Therefore, provisions must be provided to limit such cantilever wall movements by installing upper levels of supports during early stages of excavation to avoid potentially damaging ground movements, especially for flexible walls. The effect of depth of cantilever excavation  $H_{un}$  on wall and ground movements is illustrated in Figure 9. The depth of cantilever excavation  $H_{un}$  was controlled in the analyses by varying the depth at which the top most support is installed while other variables being kept constant, and therefore, the differences in the wall and ground movements between the different cases solely reflect the effect of  $H_{un}$ . For example, the differences in the wall and ground movements profiles for  $H_{un}=1$  and 4 m are due to the effect of the cantilever-type wall movement. As seen in Figure 9, it appears that the wall and ground movements are significantly reduced by keeping  $H_{un}=3$  m or less, and that the depth of cantilever excavation  $H_{un}$  only affects the profiles within the zone approximately  $0.3H$  from the edge of excavation. This has important implications on potential damage to buildings and buried pipelines located relatively close to the edge of excavation. Potentially damaging ground movements to these buildings and utilities can be avoided if a strict provision is implemented on  $H_{un}$  during early stages of excavation.

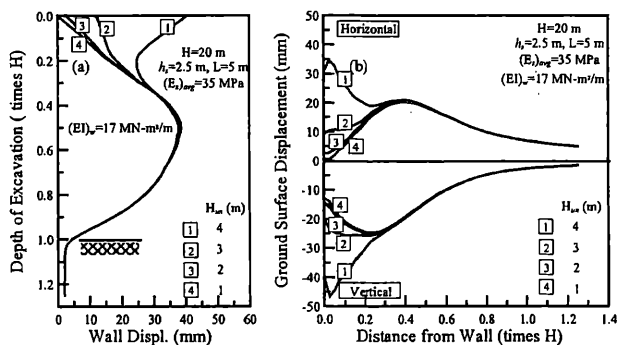


Figure 9. Variation of wall and ground movements with  $H_{un}$ .

Examples of which how the excavation depth below a lower-most support influences wall and ground surface movements for a given wall stiffness are illustrated in Figure 10. As shown in Figure 10, the effect of increase in  $L$  would be to increase the lateral bulging of the wall, implying that a significant portion of wall movements, and thus ground movements, can be reduced by limiting the excavation depth  $L$  to a minimum during construction. Fur-

thermore, it is of interest to note that an increase in the lateral wall bulging tends to modify the shape of settlement profile from parabolic to concave downward. The volume and the slope of the ground surface displacement profile also appear to be decreased by an order of more than two when decreasing  $L$  from 6 m to 3 m. The results demonstrate that excavation procedure during construction requires careful scrutiny to limit potentially damaging ground movements.

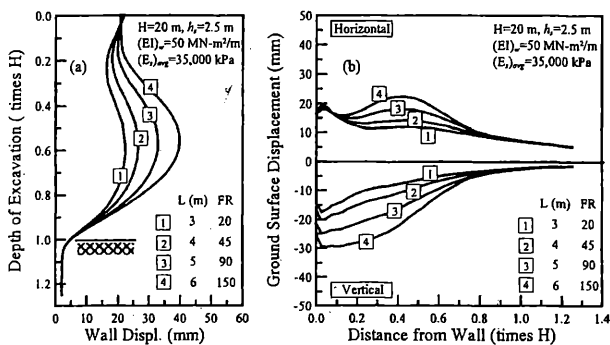


Figure 10. Variation of wall and ground movements with  $L$ .

#### 4.3 Normalized ground surface displacement profiles

In view of ground movement prediction, it would be desirable if normalized relationships can be established among different conditions. Inspection of the normalized ground surface displacement profiles for cases with a same flexibility ratio but with different combinations of  $(EI)_w$ ,  $E_s$ , and  $L$  indicate no appreciable variation, suggesting that the flexibility ratio can be used as a common index relating relative stiffness of wall system to ground movement profiles. Note that the depth of cantilever excavation  $H_{un}$  was used when calculating the flexibility ratio for the cantilever excavation stages.

Figure 11 presents the ground surface displacement profiles normalized with their maximum values for the cantilever and lateral bulging stages, in which a range of profiles having different flexibility ratios are included. The flexibility ratios covered in this figure bracket a wide range of cases frequently encountered in practice, and therefore, the profiles can be used to make a first order estimate of ground movements for a given excavation. Although there appears to exist some variation in the normalized curves for a given FR, this scatter has little practical significance since the order of magnitude of the movements in the region of scatter are usually small, i.e.,  $< 0.5$  cm. Ground surface displacement profiles for any deep excavation can thus be estimated using the normalized profiles in Figure 11 and the flexibility ratio. A two-step approach can be adopted for ground movement prediction, in which components from the cantilever and lateral bulging stages, are systematically determined from Figures 11a and 11b,

respectively. Adding the two components would then yield the final ground surface displacement profiles for a given excavation.

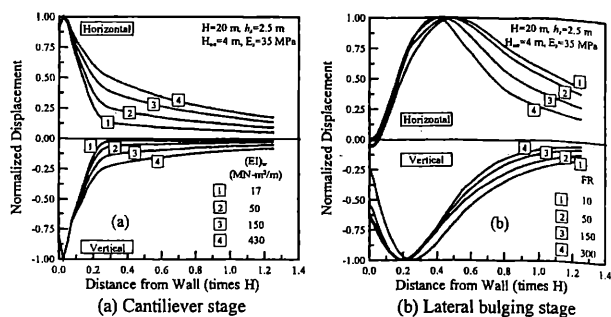


Figure 11. Normalized ground surface displacement profiles

## 5 CONCLUSIONS

Deep-excavation induced ground movement characteristics are presented based on the results of numerical investigation. A finite element model, validated against available large-scale tieback model test, was employed and a parametric study was performed on variables influencing wall and ground movements. Based on the results, sources of wall movements are identified and ground movement characteristics are related to the sources of wall movements. Normalized ground surface displacement profiles for use in a first order prediction of deep excavation-induced ground surface displacements are presented.

## ACKNOWLEDGEMENTS

This research was supported by SAFE (SAFETY and Structural Integrity Research Center) at Sungkyunkwan University. The financial support is gratefully acknowledged.

## REFERENCES

- ABAQUS (ver. 5.8) 1999. Hibbit, Karlsson & Sorensen, Inc.
- Boscardin, M.D. and Cording, E.J. 1987. Building Response to Excavation-Induced Settlement. *Journal of Geotechnical Engineering*, ASCE, Vol. 115, No. 1, pp. 1-21.
- Burland, J.B. 1995. Assessment of risk of damage to buildings due to tunneling and excavation. *Proc. 1<sup>st</sup> Int. Conf. On Earthquake Geotechnical Engineering*, IS-Tokyo, 14pp.
- Cording, E.J. 1985. Evaluation and control of ground movements around tunnels and excavations in soil. *XII Int. Conf. on Soil Mechanics and Foundation Engineering*, San Francisco, California, pp. 106-131.
- Cording, E.J. and O'Rourke, T.D. 1977. Excavation, Ground Movements, and Their Influence on Buildings. *Protection of Structures Adjacent to Braced Excavation*, ASCE Annual Convention, San Francisco (preprint)
- Mueller, C. 2000. *Load and Deformation Response of Tieback Walls*. Ph.D. Thesis, Univ. of Illinois at Urbana-Champaign
- Rowe, P.W. 1962. *The stress-dilatancy relation for static equilibrium of an assembly of particles in contact*, Proc. Roy. Soc. London A269, pp. 500-527.